J Mater Sci (2011) 46:3855–3861
DOI 10.1007/s10853-011-5306-1

# Ab initio study of structural, electronic, phase diagram, and optical properties of $CdSe_xTe_{1-x}$ semiconducting alloys

**S. Ouendadji · S. Ghemid · N. Bouarissa · H. Meradji · F. El Haj Hassan**

Received: 9 October 2010 / Accepted: 18 January 2011 / Published online: 1 February 2011


**Abstract** Based on the self-consistent ab initio full potential-linearized augmented plane wave method, the structural, electronic, optical, and thermodynamic properties of $CdSe_xTe_{1-x}$ ternary semiconductor alloys have been investigated. The exchange–correlation potential was calculated using both the generalized gradient approximation (GGA) by Perdew–Burke–Ernzerhof (PBE) and the GGA by Engel–Vosko (EV-GGA). The ground-state properties are determined for the cubic bulk materials CdSe, CdTe, and their mixed crystals at various concentrations ($x = 0.25$, 0.5, and 0.75). Deviation of the lattice parameter from Vegard's law and the bulk modulus from linear concentration dependence has been examined. The microscopic origins of the band-gap bowing parameter have been discussed. Moreover, the refractive index and the optical dielectric constant for $CdSe_xTe_{1-x}$ are studied using different models. Besides, the thermodynamic stability of the alloys of interest is investigated by means of the miscibility critical temperature.

S. Ouendadji · S. Ghemid · H. Meradji
Laboratoire de Physique des Rayonnements, Département de Physique, Faculté des Sciences, Université de Annaba, Annaba, Algeria

N. Bouarissa (✉)
Department of Physics, Faculty of Science, King Khalid University, P. O. Box 9004, Abha, Saudi Arabia
e-mail: n_bouarissa@yahoo.fr

F. El Haj Hassan
Laboratoire de Physique des Matériaux, Faculté des Sciences, Université Libanaise, El-hadath, Beirut, Lebanon

## Introduction

The II–VI compound semiconductors belonging to the cadmium chalcogenides family have recently received considerable interest from both theoretical and experimental point of views. This is because of their specific physical properties. Among them, the cadmium chalcogenides CdX (X = S, Se, and Te) have been reported by several authors [1–10]. These materials have important applications in photo-electrochemical devices. They are characterized by different degrees of covalent, ionic, and metallic bonding, and they crystallize in different crystal structures (such as zinc-blende and wurtzite). In this study, the zinc-blende phase is adopted. To take advantage of them, it requires a thorough knowledge of their properties that are important for the evaluation of their expectable domain of applications.

Based on the ab initio self-consistent full potential-linearized augmented plane wave (FP-LAPW) method, this article reports a theoretical investigation of the structural, electronic, optical, and thermodynamic properties of CdSe, CdTe, and their ternary alloys $CdSe_xTe_{1-x}$. To the best of the knowledge, no experimental work has been conducted so far for the mixed crystals of interest in the composition range 0–1. However, on the theoretical side, few attempts have been made for predicting their physical properties [11]. This has prompted the authors to take such a calculation on such alloys of interest.

The article is organized as follows: In "Introduction" section, a brief introduction was given. In "Methods of calculation" section, the authors describe the computational technique that has been adopted for the calculations. The authors present the results and discuss them in "Results and discussion" section. Finally, this study is summarized in "Conclusion" section.

## Method of calculation

All calculations were performed using the FP-LAPW method [12] within the frame work of the density functional theory (DFT) [13, 14] as implemented in the WIE2K code [15]. The exchange–correlation potential for structural properties was calculated by the generalized gradient approximation (GGA) based on Perdew et al. [16], while for electronic properties in addition to that, the Engel-Vosko (EV-GGA) [17] scheme was applied. In the FP-LAPW method, the wave function and potential are expanded in spherical harmonic functions inside non-overlapping spheres surrounding the atomic sites (muffin-tin spheres). The convergence parameter $R_{MT}k_{max}$, which controls the size of the basis sets in these calculations, was set to 9. $R_{MT}$ denotes the smallest atomic sphere radius and $k_{max}$ gives the magnitude of the largest $k$ vector in the plane wave expansion. The charge density was Fourier expanded up to $G_{max}$. The $G_{max}$ parameter was taken to be 14.0 Bohr$^{-1}$. The Cd ([Kr] $4d^{10}$ $5s^2$), Se ([Ar] $3d^{10}$ $4s^2$ $4p^2$), and Te ([Kr] $4d^{10}$ $5s^2$ $5p^4$) states are treated as valence electrons. The $R_{MT}$ are taken to be 2.3, 2.2, and 2.4 atomic units (a.u.) for Cd, Se, and Te, respectively. Meshes of 73 $k$-points were chosen in the whole Brillouin zone for CdTe and CdSe. For $CdSe_xTe_{1-x}$ ternary alloys, 125 special $k$-points were chosen.

## Results and discussion

### Structural properties

The authors first calculated the structural properties of CdSe, CdTe compounds, and their ternary alloys in the zinc-blende phase using the GGA scheme. The alloys are modeled at some selected compositions with ordered structures described in terms of periodically repeated supercells. For the compositions $x = 0.25$, 0.5, and 0.75, the simplest structure is an eight- atom simple cubic lattice. The total energy has been calculated as a function of unit cell volume and is fitted to the Murnaghan's equation of state [18]. This allowed the obtaining of the equilibrium structural properties such as the lattice constant ($a$) and the bulk modulus ($B$). The GGA-calculated structural parameters for $CdSe_xTe_{1-x}$ at various compositions $x$ are listed in Table 1. In this table, comparison is made with experimental and previous theoretical values of the lattice constant and bulk modulus (all at zero pressure). In view of Table 1, one can note that the results regarding the lattice constant for CdTe and CdSe are overestimated with respect to the experimental values reported in [19, 20]; the GGA is expected to overestimate slightly the lattice constant [21, 22]. For CdSe, the agreement between the calculated and experimental values of $a_0$ is slightly worse than for CdTe. For compositions in the range 0–1, the results are predictions and seem likely to be useful as a reference for future experimental work.

**Table 1** Calculated lattice parameter ($a$) and bulk modulus ($B$) for $CdSe_xTe_{1-x}$ ($0 \le x \le 1$) at equilibrium volume

| Composition $x$ | Lattice parameter $a$ (Å) | | Bulk modulus $B$ (GPa) | | Other cal. |
|---|---|---|---|---|---|
| | This study | Exp. | This study | Exp. | |
| 0 | 6.631 | 6.48[a] | 33.793 | 39[a] | 44.5[c] |
| 0.25 | 6.532 | | 38.864 | | |
| 0.50 | 6.438 | | 40.864 | | |
| 0.75 | 6.331 | | 43.549 | | |
| 1 | 6.216 | 6.05[b] | 44.86 | | |

[a] Ref. [19]

[b] Ref. [20]

[c] Ref. [25]

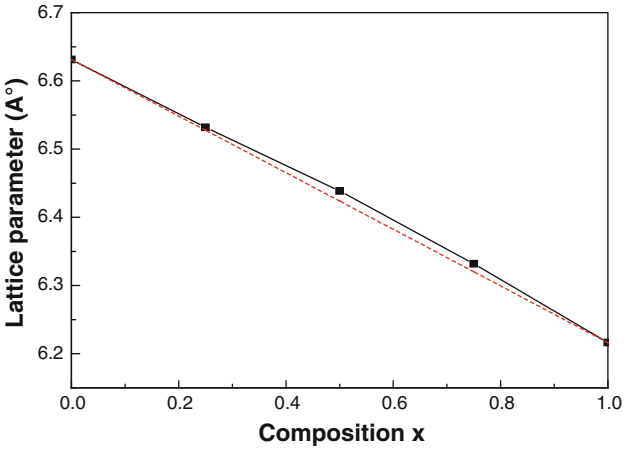


**Fig. 1** Composition dependence of the calculated lattice constant (*solid squares*) for $CdSe_xTe_{1-x}$ alloys compared with Vegard's law (*dashed line*)

The composition dependence of the calculated lattice constant for $CdSe_xTe_{1-x}$ ternary alloys is shown in Fig. 1. Note that as the composition $x$ increases the lattice constant decreases monotonically and almost linearly exhibiting an upward weak bowing parameter of −0.051 Å. The linear behavior of the lattice constant is consistent with the Vegard's law [23] that is often used by researchers for obtaining the lattice constant of zinc-blende semiconductor alloys [5, 24]. This is clearly seen in Fig. 1. Thus, one can conclude that the deviation from Vegard's law for the lattice constant regarding the normal substitution for $CdSe_xTe_{1-x}$ ternary alloys is negligible. This fact suggests that there is a good agreement between the DFT predictions and the linear Vegard's law.

The ratio of the change of pressure to the fractional volume compression is called the bulk modulus ($B$) of the material. The calculated $B$'s for CdTe, CdSe, and some of their mixed crystals $CdSe_xTe_{1-x}$ are depicted in Table 1. To the knowledge, the only available experimental value of $B$ for parent compounds of interest is that for CdTe. The value of $B$ for CdTe as illustrated by the results is smaller than the experimental result reported in Ref. [19]. In terms of theoretical results, the B for CdTe is also underestimated with respect to that reported by Zerroug et al. [25]. For other compositions rather than 0, the results are predictions. It is worth noting that as the chalcogenide atomic number increases the bulk modulus of cadmium chalcogenide compound decreases which makes the material more compressible.

The variation of the bulk modulus as a function of the alloy composition x for $CdSe_xTe_{1-x}$ ternary mixed crystals as illustrated by the results is displayed in Fig. 2. Also shown for comparison is the variation of $B$ versus $x$ predicted by a linear concentration dependence (LCD) method (Fig. 2, dashed line). Note that as the composition increases, $B$ increases as well. The enhancement of $B$ versus $x$ is monotonic. This indicates that the material under load becomes less compressible when increasing the alloy composition $x$. However, in contrast to the lattice constant, the bulk modulus varies non-linearly with respect to $x$ exhibiting a large upward bowing parameter of $-7.811$ GPa. This makes a deviation from LCD very significant.

## Electronic properties

The electronic band structure of the materials of interest has been calculated using both the GGA and the EV-GGA schemes. Even the EV-GGA functional was used so as to calculate the energy band-gaps; this approximation was not used for the optimization of the lattice constant. The latter was optimized by using the PBE-GGA functional approach. In this respect, the fundamental band-gap energy ($E_\Gamma^\Gamma$) has been obtained for $CdSe_xTe_{1-x}$ at various compositions $x$ ranging from 0 to 1. The results are listed in Table 2. Also shown for comparison are the available data in the literature. The calculated band-gap energies $E_\Gamma^\Gamma$ are underestimated by the GGA. Although the GGA calculations severely underestimate the band gap at Γ, the calculated trends are correct. The band gap at Γ of the CdTe structure is larger than the CdSe structure. It is worth noting that the calculated values of $E_\Gamma^\Gamma$ via EV-GGA approach are highly improved with respect to experiment as compared to those obtained via GGA. Besides, the EV-GGA results are in better agreement with experiment than the previous theoretical data reported in Refs. [20, 26]. As a matter of fact, the simple form of the GGA is not sufficiently flexible for accurately reproducing both exchange–correlation energy and its charge derivative [25]. By considering this short coming, Engel and Vosko [17] have constructed a new functional form of the GGA that was able to better reproduce the exchange potential at the expense of less agreement as regards exchange energy when compared to experiment.

The variation of $E_\Gamma^\Gamma$ as a function of the composition x for the material of interest obtained by using GGA and EV-GGA approaches is shown in Fig. 3. The GGA results show that going from $x = 0$ to $x = 1$, $E_\Gamma^\Gamma$ decreases monotonically in $CdSe_xTe_{1-x}$ system. The situation concerning the EV-GGA results is quite different where one can notice that $E_\Gamma^\Gamma$increases monotonically with increasing the composition $x$. By fitting the $E_\Gamma^\Gamma$energy gaps data for both GGA and EV-GGA approaches using a least squares procedure, the following analytical expressions have been obtained,

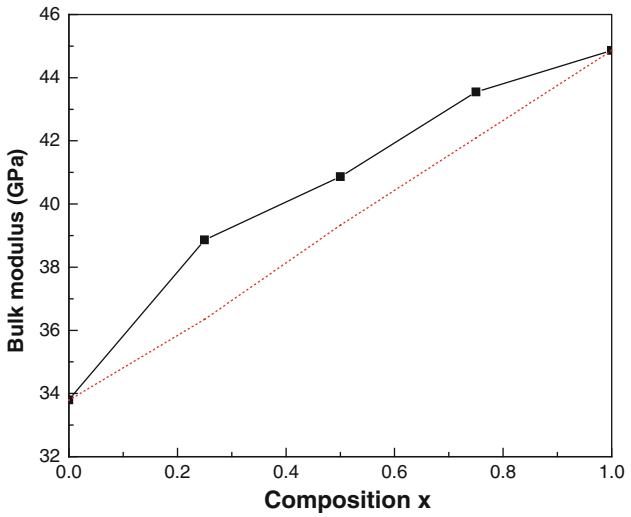


**Fig. 2** Composition dependence of the bulk modulus of $CdSe_xTe_{1-x}$ alloys (*solid squares*) compared with LCD prediction (*dashed line*)

**Table 2** Band-gap energies of zinc-blende $CdSe_xTe_{1-x}$ alloys at various concentrations $x$

| Composition $x$ | Band-gap energy (eV) | | | | |
|---|---|---|---|---|---|
| | GGA | Exp. | Other cal. | | EVGGA |
| 0 | 0.588 | 1.92[a] | 0.62[a] | 0.88[b] | 1.087 |
| 0.25 | 0.549 | | | | 1.13 |
| 0.50 | 0.512 | | | | 1.17 |
| 0.75 | 0.492 | | | | 1.18 |
| 1 | 0.475 | 1.90[a] | 0.48[a] | 0.73[b] | 1.2 |

[a] Ref. [20]

[b] Ref. [26]

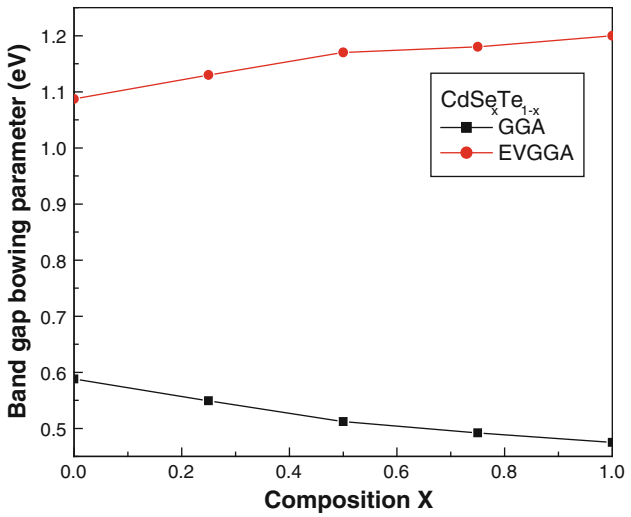


**Fig. 3** Composition dependence of the calculated band gap energy $E_\Gamma^\Gamma$ using GGA and EV-GGA for $CdSe_xTe_{1-x}$

$$E_\Gamma^\Gamma(x) = 0.59 - 0.18x + 0.07x^2 \qquad \text{(GGA)} \qquad (1)$$

$$E_\Gamma^\Gamma(x) = 1.09 + 0.20x - 0.08x^2 \qquad \text{(EV} - \text{GGA)} \qquad (2)$$

The quadratic terms are refereed to as band-gap bowing parameters. The bowing parameter of $CdS_xTe_{1-x}$ [25] appear to be larger than that of $CdSe_xTe_{1-x}$. This is due presumably to the lattice mismatch, that is larger in $CdS_xTe_{1-x}$ ($\Delta a = 0.66$ Å) as compared to $CdSe_xTe_{1-x}$ ($\Delta a = 0.43$ Å). This could be also understood in terms of the difference in the electro-negativity between Te, S, and Se atoms which is according to the Pauling scale 2.58 for S, 2.1 for Te, and 2.55 for Se.

In order to better understand the physical origins of the band-gap bowing in these alloys, we have followed the procedure of Bernard and Zunger [27], in which the bowing parameter ($b$) is decomposed into three physically distinct contributions. In fact the overall band-gap bowing coefficient at $x = 0.50$ measures the change in the band-gap according to the reaction:

$$AB(a_{AB}) + AC(a_{AC}) \rightarrow AB_{0.50}C_{0.50}(a_{eq}) \qquad (3)$$

Where $a_{AB}$ and $a_{AC}$ are the equilibrium lattice constants of the binary compounds AB and AC, respectively; $a_{eq}$ is the alloy equilibrium lattice constant. The authors now decompose the previous reaction into three steps:

$$AB(a_{AB}) + AC(a_{AC}) \xrightarrow{VD} AB(a) + AC(a) \qquad (4)$$

$$AB(a) + AC(a) \xrightarrow{CE} AB_{0.50}C_{0.50}(a) \qquad (5)$$

$$AB_{0.50}C_{0.50}(a) \xrightarrow{SR} AB_{0.50}C_{0.50}(a_{eq}) \qquad (6)$$

The first step measures the volume deformation (VD) effect on the bowing parameter. The corresponding contribution of VD to the total band-gap bowing parameter represents the relative response of the band structure of the binary compounds AB and AC to hydrostatic pressure, which arises here from the change of their individual equilibrium lattice constants with respect to the alloy value $a = a(x)$ (Vegard's rule). The second contribution is that comes from the charge-exchange (CE) contribution $b_{CE}$ which reflects a charge transfer effect due to the different (averaged) bonding behavior at the lattice constant $a$. The last contribution denoted by $b_{SR}$ measures the change due to the structural relaxation (SR) in passing from the unrelaxed to the relaxed alloy. Consequently, the total band-gap bowing parameter is defined as,

$$b = b_{VD} + b_{CE} + b_{SR} \qquad (7)$$

where

$$b_{VD} = 2[\varepsilon_{AB}(a_{AB}) - \varepsilon_{AB}(a) + \varepsilon_{AC}(a_{AC}) - \varepsilon_{AC}(a)] \qquad (8)$$

$$b_{CE} = 2[\varepsilon_{AB}(a) + \varepsilon_{AC}(a) - 2\varepsilon_{ABC}(a)] \qquad (9)$$

$$b_{SR} = 4[\varepsilon_{ABC}(a) - \varepsilon_{ABC}(a_{eq})] \qquad (10)$$

where $\varepsilon$ is the energy gap that is calculated for the indicated atomic structures and lattice constants. The energy band-gap terms in Eqs. 8–10 are calculated separately with self-consistent band structure FP-LAPW within both GGA and EV-GGA approaches. Our results concerning the different bowing parameters, namely $b_{VD}$, $b_{CE}$ and $b_{SR}$ are collected in Table 3 along with the band-gap bowing parameters obtained in Eqs. 1 and 2 using a quadratic fit. From Table 3, one can note that the contribution of $b_{CE}$ to $b$ in the alloys under load is larger than that of $b_{SR}$ to $b$. It should be also noted that the contribution of $b_{VD}$ to b is negative, i.e., it decreases the value of b. It was observed that using Bernard and Zunger approach, the b estimated by the EV-GGA is larger in magnitude than that obtained by the GGA.

## Thermodynamic properties

Let us now turn our attention to the phase stability of $CdSe_xTe_{1-x}$ ternary alloys. For this purpose, the authors calculate the Gibbs free energy of mixing $\Delta G_m(x,T)$which allows to access the $T$–$x$ phase diagram and obtain the critical temperature $T_c$. More details about the calculations are given in Refs. [28, 29].

**Table 3** Decomposition of optical bowing into volume deformation (VD), charge exchange (CE), and structural relaxation (SR) contributions compared with the typical bowing obtained by a quadratic fit

| GGA | | | | | EV-GGA | | | |
|---|---|---|---|---|---|---|---|---|
| $b_{VD}$ | $b_{CE}$ | $b_{SR}$ | $B$ | $b$ | $b_{VD}$ | $b_{CE}$ | $b_{SR}$ | $b$ |
| −0.70 | 0.65 | 0.07 | 0.02 | 0.07 | 0.15 | 0.7 | −0.17 | −0.08 |

All bowing parameters are expressed in eV

The Gibbs free energy of mixing, $\Delta G_m$ for an alloy is expressed as

$$\Delta G_m = \Delta H_m - T\Delta S_m \quad (11)$$

where

$$\Delta H_m = \Omega x(1-x) \quad (12)$$

$$\Delta S_m = -R[x\ln x + (1-x)\ln(1-x)] \quad (13)$$

$\Delta H_m$ and $\Delta S_m$ are the enthalpy and the entropy of mixing, respectively; $\Omega$ is the interaction parameter, $R$ is the gas constant, and $T$ is the absolute temperature. Only the interaction parameter $\Omega$ depends on the material properties. The mixing enthalpy of alloys can be obtained as the difference in energy between the alloy and the weighted sum of the constituents [29]:

$$\Delta H_m = E_{AB_xC_{1-x}} - xE_{AB} - (1-x)E_{AC} \quad (14)$$

where$E_{AB_xC_{1-x}}$, $E_{AB}$ and $E_{AC}$ are the energies of $AB_xC_{1-x}$, AB and AC materials, respectively. The authors then calculate $\Delta H_m$ to obtain the interaction parameter $\Omega$ as a function of the alloy concentration x.

The variation of $\Omega$ as a function of the composition x for $CdSe_xTe_{1-x}$ ternary alloys has been determined. The best fit of our data regarding $\Omega$ is found to be linear yielding the following expression,

$$\Omega(x) = 64.91 - 4.76x \quad (15)$$

where $\Omega$ is expressed in kcal/mol. The average value of $\Omega$ obtained in this study in the composition range $0 \leq x \leq 1$ is estimated to be 62.53 kcal/mol.

In order to determine the stable, metastable and unstable mixing regions of the alloy of interest, we have calculated the temperature-composition phase diagram. Our results are displayed in Fig. 4. At a temperature lower than the critical temperature $T_c$, the two bimodal points are determined as those points at which the common tangent line touches the $\Delta G_m$ curves, whereas the two spinodal points are determined as those points at which the second derivative of $\Delta G_m$ is zero. A critical temperature ($T_c$) value of 899.57 K has been evaluated for $CdSe_xTe_{1-x}$. The equilibrium solubility limit, i.e., the miscibility gap is marked by the spinodal curve in the phase diagram. For temperatures and compositions above this curve a homogeneous alloy is predicted. One can also note the existence of a wide range between spinodal and binodal curves indicating thus that $CdSe_xTe_{1-x}$ may have a metastable phase.

## Optical properties

The refractive index ($n$) of semi-conducting materials is very important in determining the optical and electric properties of the crystal. Knowledge of $n$ is essential in the design of heterostructure lasers and in optoelectronic devices. In the present study, $n$ has been obtained using different models that are related to the fundamental energy band-gap.

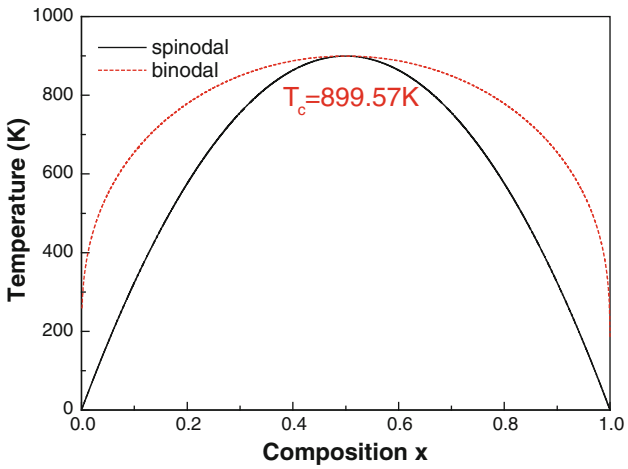


**Fig. 4** $T$–$x$ phase diagram of $CdSe_xTe_{1-x}$ alloys. *Dashed line* binodal curve. *Solid line* spinodal curve

(i). The Moss formula [30] based on an atomic model

$$E_g n^4 = k \quad (16)$$

where $E_g$ is the energy band-gap and $k$ is a constant. The value of $k$ as reported in Ref. [30] is 108 eV.

(ii). The Ravindra et al. [31] expression,

$$n = \alpha + \beta E_g \quad (17)$$

with $\alpha = 4.084$ and $\beta = -0.62$ eV$^{-1}$.

(iii). Herve and Vandamme's empirical relation [32],

$$n = \sqrt{1 + \left(\frac{A}{E_g + B}\right)^2} \quad (18)$$

with $A = 13.6$ and $B = 3.4$ eV.

Based on the electronic structure calculated from FP-LAPW method, the dielectric function $\varepsilon(\omega) = \varepsilon_1(\omega) + i\varepsilon_2(\omega)$ has been calculated, where $\varepsilon_1(\omega)$ and $\varepsilon_2(\omega)$ are the real and imaginary parts of $\varepsilon(\omega)$, respectively. By knowing the values of $\varepsilon_1(\omega)$, $\varepsilon_2(\omega)$, and $\varepsilon(\omega)$, the refractive index $n$ has also been calculated using the expression,

$$n(\omega) = \left[\frac{\varepsilon(\omega)}{2} + \frac{\sqrt{\varepsilon_1^2(\omega) + \varepsilon_2^2(\omega)}}{2}\right]^{\frac{1}{2}} \quad (19)$$

The results for CdSe, CdTe and some of their ternary alloys are listed in Table 4. Comparison with the known data has been made where possible. As compared with the other relations used, it seems that the values of $n$ obtained from FP-LAPW method for the end-point compounds (i.e., CdSe and CdTe) are in better agreement with the known data. The reason lies in the fact that relations (16)–(18) from which $n$ is estimated depend on the fundamental band

**Table 4** Refractive indices of $CdSe_xTe_{1-x}$ for different composition $x$

| Composition $x$ | n (calculated from (16)) | n (calculated from (17)) | n (calculated from (18)) | Present FP-LAPW | Known | |
|---|---|---|---|---|---|---|
| 0 | 3.68 | 3.72 | 3.55 | 2.46 | 2.92[a] | 2.72[b] |
| 0.25 | 3.75 | 3.74 | 3.59 | 2.57 | | |
| 0.5 | 3.81 | 3.77 | 3.62 | 2.44 | | |
| 0.75 | 3.85 | 3.78 | 3.63 | 2.41 | | |
| 1 | 3.88 | 3.79 | 3.65 | 2.29 | 2. 83[a] | 2.5[c] |

[a] Ref. [11]

[b] Ref. [37]

[c] Ref. [38]

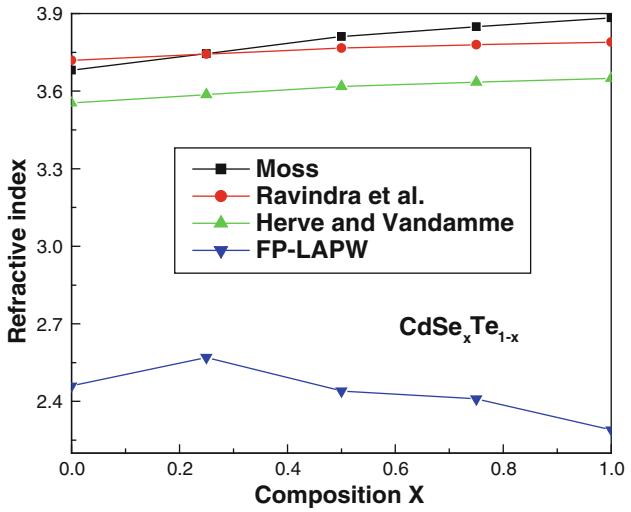


**Fig. 5** Refractive index as a function of composition $x$ for $CdSe_xTe_{1-x}$

gap energy $E_g$ that is underestimated by the GGA approach. So it is clear that the deficiency is in the band gap value rather than in the models themselves. The better agreement of the electronic structure based optical properties with experimental values is typical of the response function method used in WIEN, largely due to the underestimation of the band gap value. For lack of both experimental and theoretical data in the literature from $n$ of $CdSe_xTe_{1-x}$in the composition range $0 < x < 1$, this results stand, therefore, as predictions for the refractive index.

The variation of $n$ as a function of composition x for $CdSe_xTe_{1-x}$ is shown in Fig. 5. Note that $n$ increases monotonically with increasing $x$ for all empirical methods. However, the use of the FP-LAPW leads to a non-monotonic behavior of $n$. The behavior of $n$ based on empirical models is consistent with the fact that the smaller $E_g$ gap material has a large value of $n$ as generally reported for other semiconductor alloys [33–35].

Based on the FP-LAPW calculated values of $n$ (which are the most accurate ones among the other used models),

**Table 5** Optical high-frequency dielectric constant of $CdSe_xTe_{1-x}$ for different composition $x$

| Composition $x$ | Present FP-LAPW | Known data | | |
|---|---|---|---|---|
| 0 | 6.08 | 7.2[a] | 9.02[b] | 6.70[c] |
| 0.25 | 6.60 | | | |
| 0.50 | 5.95 | | | |
| 0.75 | 5.81 | | | |
| 1 | 5.25 | 5.68[b] | 6.26[c] | 5.8[d] |

[a] Ref. [39]

[b] Ref. [36]

[c] Ref. [40]

[d] Ref. [41]

the high-frequency dielectric constant ($\varepsilon_\infty$) has been obtained for different compositions $x$ using the following expression,

$$\varepsilon_\infty = n^2 \tag{20}$$

The results along with the known data in the literature are given in Table 5. As compared with the known data, our results seem to be in good agreement with the data reported in Ref. [36]. No available data concerning $\varepsilon_\infty$ have been reported in the literature for $CdSe_xTe_{1-x}$ $(0 < x < 1)$, to the knowledge. Hence, no comment for the time being can be ascribed to the accuracy of our results in this range. By fitting our FP-LAPW $\varepsilon_\infty$ data using a least-squares procedure, we have obtained the following analytical expression,

$$\varepsilon_\infty(x) = 6.16 + 1.48x - 2.77x^2 \tag{21}$$

This expression can be used to predict the $\varepsilon_\infty$ for any $x$ in the material of interest.

## Conclusion

The FP-LAPW method within the DFT in the frame work of GGA and EV-GGA schemes have been used to calculate

structural, electric, thermodynamic and optical properties of $CdSe_xTe_{1-x}$ mixed crystals ($0 \leq x \leq 1$) in the zinc-blende phase. A summary of the key findings follows.

(i). The deviation from Vegard's law for the lattice constant regarding the normal substitution for $CdSe_xTe_{1-x}$alloys is negligible.

(ii). The bulk modulus of cadmium chalcogenide compounds decreases with increasing the chalcogenide atomic number indicating thus that the material under load becomes more compressible.

(iii). The microscopic origins of the band-gap bowing parameter for $CdSe_xTe_{1-x}$ were determined.

(iv). The calculated phase diagram indicated that $CdSe_xTe_{1-x}$is stable at temperature of 899.57 K.

(v). The refractive indices calculated with the use of FP-LAPW method were found to be in better agreement with the known data than those calculated from empirical relations.

## References


1. Tomasulo A, Ramakrishna MV (1996) J Chem Phys 105:3612
2. Nelmes RJ, McMohan MI (1998) Semicond Semimater 54:145
3. Lee G-D, Lee MH, Ihm J (1995) Phys Rev B 52:1459
4. Deligoz E, Colakoglu K, Ciftci Y (2006) Physica B 373:124
5. Bouarissa N (2007) Physica B 399:126
6. Hannachi L, Bouarissa N (2009) Physica B 404:3650
7. Wei S, Zhang SB (2000) Phys Rev B 62:6944
8. Cote′ M, Zakharov O, Rubio A, Cohen ML (1997) Phys Rev B 55:13025
9. Zakharov O, Rubio A, Blase X, Cohen ML, Loui SG (1994) Phys Rev B 50:10780
10. Mujica A, Rubio A, Munoz A, Needs RJ (2003) Rev Mod Phys 75:863
11. Hannachi L, Bouarissa N (2008) Superlattice Microstruct 44:794
12. Koelling DD, Harmon BN (1977) J Phys C 10:3107
13. Hohenberg P, Kohn W (1964) Phys Rev 136:B864
14. Kohn W, Sham LJ (1965) Phys Rev 140:A1133
15. Blaha P, Schwarz K, Madsen GKH, Kvasnicka D, Luitz J (2001) WIEN2K, an augmented plane wave + local orbitals program for calculating crystal properties, Karlheinz Schwarz, Techn. Universitat, Wien. ISBN 3-9501031-1-2
16. Perdew JP, Burke S, Ernzerhof M (1996) Phys Rev Lett 77:3865
17. Engel E, Vosko SH (1993) Phys Rev B 47:13164
18. Murnaghan FD (1944) Proc Natl Acad Sci USA 30:244
19. Madelung O, Schlz M, Weiss H (eds) (1982) Landolt-Borstein: numurical data and functional relationships in science and technology, vol 17. Springer, Berlin
20. Heyd J, Peralta JE, Scuseria GE (2005) Chem Phys 123:1
21. Saib S, Bouarissa N (2005) Eur Phys J B 47:379
22. Zerroug S, Ali Sahraoui F, Bouarissa N (2009) Philos Mag B 89:1611
23. Vegard L (1921) Z Phys 5:17
24. Bouarissa N (1998) Phys Lett A 245:285
25. Zerroug S, Ali Sahraoui F, Bouarissa N (2007) Eur Phys J B 57:9
26. Peralta JE, Uddin J, Scuseria GE (2005) J Chem Phys 122: 084108
27. Bernard JE, Zunger A (1986) Phys Rev B 34:5992
28. Swalin RA (1961) Thermodynamics of solids. Wiley, New York
29. Teles LK, Furthmuller J, Scolfaro LMR, Leite JR, Bechstedt F (2000) Phys Rev B 62:2475
30. Gupta VP, Ravindra NM (1980) Phys Stat Sol (b) 100:715
31. Ravindra NM, Auluck S, Srivastava VK (1979) Phys Stat Sol (b) 93:k155
32. Herve PJL, Vandamme LKJ (1994) Infrared Phys Technol 35:609
33. Adachi S (1987) J Appl Phys 61:4869
34. Bouarissa N (2001) Mater Sci Eng B 86:53
35. Bouarissa N (2001) Mater Chem Phys 72:387
36. Huang MZ, Ching WY (1993) Phys Rev B 47:9449
37. D. W. Palmer www.semiconductors.co.uk
38. Singh J (ed) (1993) Physics of semiconductors and their heterostructures, Mc Graw-Hill, New York, p 84
39. Marple DTF (1964) J Appl Phys 35:539
40. Kootstra F, De Boeij PL, Snijders JG (2000) Phys Rev B 62:7071
41. Manabe A, Mitsuishi A, Yoshinaga H (1967) Jpn J Appl Phys 6:593